Pharmaceutical Research, Vol. 26, No. 8, August 2009 (© 2009)
DOI: 10.1007/s11095-009-9912-4

Research Paper

Skin Solubility Determines Maximum Transepidermal Flux for Similar Size Molecules

Qian Zhang,[1,2] Jeffrey E. Grice,[1] Peng Li,[1] Owen G. Jepps,[3] Guang-Ji Wang,[2] and Michael S. Roberts[1,4,5]

Received March 2, 2009; accepted May 11, 2009; published online June 5, 2009

Purpose. The maximum flux of solutes penetrating the epidermis has been known to depend predominantly on solute molecular weight. Here we sought to establish the mechanistic dependence of maximum flux on other solute physicochemical parameters.
Methods. Maximum fluxes, stratum corneum solubilities and estimated diffusivities through human epidermis were therefore determined for 10 phenols with similar molecular weights and hydrogen bonding but varying in lipophilicity.
Results. Maximum flux and stratum corneum solubilities of the phenolic compounds both showed a bilinear dependence on octanol-water partition coefficient (P), with solutes having a maximum solubility in the stratum corneum when $2.7<\log P<3.1$. In contrast, lag times and diffusivities were relatively independent of P. Stratum corneum-water partition coefficients and epidermal permeability coefficients were consistent with previously reported data.
Conclusion. A key finding is that the convex dependence of maximum flux on lipophilicity arises primarily from variations in stratum corneum solubility, and not from diffusional or partitioning barrier effects at the stratum corneum–viable epidermis interface for the more lipophilic phenols. Our data support a solute structure-skin transport model for aqueous solutions in which permeation rates depend on both partitioning and diffusivity: partitioning is related to P, and diffusivity to solute size and hydrogen bonding. (199 words)

KEY WORDS: maximum flux; structure- penetration relationships; transdermal permeation.

INTRODUCTION

Transdermal delivery products are expected to account for a significant proportion of drug delivery candidate products under clinical evaluation (1). A key requirement for all transdermal or topical products is an adequate delivery to either the systemic circulation or to the skin. In this context, an understanding of the physicochemical determinants of drug-skin penetration fluxes is crucial for both the choice and design of drugs to be given by this route. Prediction of skin penetration is also important in toxicological assessment after topical exposure. One of the very early treatises in this area proposed that the maximum rate of skin penetration (now commonly expressed as maximum skin flux-J_{max}) was, perhaps, the key parameter to be used in such an assessment (2). Whereas J_{max} is defined by saturated or pure compounds applied to the skin, the majority of the work on solute structure–skin penetration relationships to date has used permeability coefficients (k_p) that are defined in the limit of infinite dilution. Indeed, some estimates of J_{max} have been derived from the product of aqueous k_p and their solubilities in water (S_{aq}) in the absence of measured J_{max} (3). The advantage of J_{max} is that, for a given compound, it is an invariant in the thermodynamic description of the penetration process; by contrast, k_p depends on the formulation applied.

Lipid-water partition coefficients, solubility, melting point and molecular size have been recognised as determinants of solute structure–skin penetration relationships in early studies published in this area (4–7). A number of authors have also shown that solute hydrogen bonding may

[1] Therapeutics Research Unit, School of Medicine, Princess Alexandra Hospital, The University of Queensland, Woolloongabba, QLD 4102, Australia.
[2] Key Lab of Drug Metabolism and Pharmacokinetics, China Pharmaceutical University, Nanjing, 210038, China.
[3] School of Biomolecular and Physical Sciences, Griffith University, Brisbane, QLD 4111, Australia.
[4] School of Pharmacy and Medical Sciences, University of South Australia, North Terrace, Adelaide, SA 5000, Australia.
[5] To whom correspondence should be addressed. (e-mail: m.roberts@uq.edu.au)

ABBREVIATIONS α/β, hydrogen-bond acidity/basicity; C_v, the concentration in the vehicle; D, diffusion coefficient; F_d, the fraction of the initial solute concentration remaining in the donor; F_r, recovered in the receptor phase as a fraction of the receptor phase solubility; HPLC, high-performance liquid chromatography; J_{max}, maximum skin flux; $J_{max,estimated}$, maximum fluxes estimated from the dilute solutions; $J_{max,observed}$, flux observed for saturated solutions; J_{SS}, steady-state flux; k_p, epidermal permeability coefficient; K_{SC}, stratum corneum-water partition coefficient; log P, logarithmic (base 10) form of octanol-water partition coefficient; P, octanol-water partition coefficient; PSA, polar surface area; S_{aq}, solute solubility in water; S_{SC}, solute solubility in the stratum corneum; t_{lag}, lag time; π, dipolarity/polarisability of solute.

impede diffusion in the stratum corneum (8–11). For example, Lien and Tong (4) used skin permeability and vasoconstriction data for different solutes to show that the lipophilicity, size and S_{aq} were important. In these studies, the main barrier for skin transport was attributed to the stratum corneum squamae (5,12), with recognition that the underlying viable epidermis and, *in vitro*, the aqueous diffusion layer (5,6,13–15), and dermis (5,16) may also contribute to the skin resistance. In the late 1970s, histochemical (17) and theoretical considerations (7,18) led to recognition that the intercellular lipid in the stratum corneum was probably the most important pathway for solute transport through stratum corneum. Kasting *et al*. (14) showed that skin penetration depended on molecular size to a greater extent than previously thought. Anderson and Raykar (19) confirmed this finding, noting that the human stratum corneum k_p of cresols and hydrocortisone esters depended not only on solute lipophilicity but also had a steep dependency on molecular size. Guy and Potts (20,21) extended this with a wide range of compounds and proposed that the nonlinearity between k_p and lipophilicity arises from the confounding effect of the larger size solutes. Further, Pugh and Hadgraft (22) have used a chemical group contribution approach to describe human skin k_p. Most recently, Wang *et al*. (23) reassessed the route of stratum corneum penetration and concluded that the transcellular pathway was dominant for most compounds, irrespective of the lipophilicity. The pathway for transport through stratum corneum however, remains controversial and a key question is the permeability of the cornified cell envelope (24), which multiphoton microscopy studies suggest is dependent on the nature of the solute and the formulation (25–27).

The literature on solute structure–J_{max} relationships is less well developed. In early work using phenols, we suggested that J_{max} was related to lipophilicity (6). We also argued that melting point may be a predictor of J_{max} (28). However, in later work, we reported that solute size was the main determinant for the J_{max} of solutes through skin in a large data set (3), being unable to show a strong dependency of J_{max} on lipophilicity. Most studies report that a parabolic relationship exists between J_{max} and lipophilicity *in vitro* in human (29,30), in hairless rat (31) and hairless mouse skin (32), and *in vivo* (33,34). However, each of these studies used solutes which varied in both lipophilicity and size. Given that the larger compounds are also the more lipophilic, it is not clear whether the decrease in J_{max} for the more lipophilic solutes arises from the increase in molecular weight, or other phenomena. Alternatives include: an altered diffusion pathway for penetration in the stratum corneum (1,5,19,23); a reduced flux due to a change from a rate-limiting diffusion process through the stratum corneum to a rate-limiting partitioning across the stratum corneum–viable epidermis interface (if solubility levels in viable epidermis are approached) (32); a dependence on the mole fraction solubility in the stratum corneum (35,36); a contribution to barrier resistance by the viable epidermis (13), dermis (5) or aqueous diffusion layers (6), and a decreased clearance from the dermis or receptor phase (37). Enhanced penetration can also be achieved by supersaturating the vehicle, leading to an enhanced partitioning into the stratum corneum, as a consequence of the antinucleating ability of the intercellular lipids of the stratum corneum (38). The skin structure and the diffusion process involved in solute penetration through the skin are schematically depicted in Fig. 1.

In this work, we sought to resolve some of the current unanswered questions defining solute structure–J_{max} relationships though skin by studying the human skin penetration for solutes from a single class (phenols) with varying lipophilicity but with approximately the same molecular weight and a S_{aq} above 0.025%. Having shown previously that additional polar groups to a phenol decrease its diffusivity (6), a finding also reported later by others (8,10,19), we limited our selection to compounds unlikely to show a significant change in stratum corneum diffusivity.

We performed two sets of *in vitro* experiments: one set to determine the solubility of solutes in water, stratum corneum, and their octanol-water partition coefficients P; and another set to determine the J_{max} of solutes through epidermis. In order to allow comparison with earlier studies (6,32,33), both saturated and dilute aqueous solutions were used. Data collected from these two sets of experiments allowed us to distinguish the relative contributions due to solute solubility, partitioning and diffusivity in the stratum corneum, as well as contributions due to other epidermal layers.

Our results show that the key determinant of J_{max} for solutes with differing lipophilicity is their S_{SC}. Furthermore, we observe the same convex trend with lipophilicity that has been observed previously, but this time for a set of compounds with the same molecular weight. This indicates that the drop in J_{max} for highly lipophilic molecules is indeed due to their lipophilicity, and independent of size considerations.

THEORY

The permeation of drugs through the skin is generally considered to be a diffusive process. By approximating the skin as a homogenous membrane, Fick's second law (the diffusion equation) can be applied to describe the nature of permeation of compounds applied in solution to the skin. Under the assumption of a constant donor concentration and sink conditions (zero receptor concentration), the time-dependent cumulative amount of drug $Q(t)$ penetrated through the membrane with area A after time t is given by:

$$Q(t) = AJ_{SS}\left[t - t_{lag} - \frac{12t_{lag}}{\pi^2}\sum_{n=1}^{\infty}\frac{(-1)^n}{n^2}\exp\left(-n^2\pi^2\frac{t}{6t_{lag}}\right)\right] \quad (1)$$

where the steady-state flux (J_{SS}) and the lag time (t_{lag}) are given by (39):

$$J_{SS} = K_{SC}DC_v/h \quad (2)$$

$$t_{lag} = h^2/6D \quad (3)$$

where C_v is the concentration in the vehicle (in this case, we use aqueous solution), D the effective diffusion coefficient, h the thickness of the stratum corneum and K_{SC} the partition coefficient of the solute between the stratum corneum and the

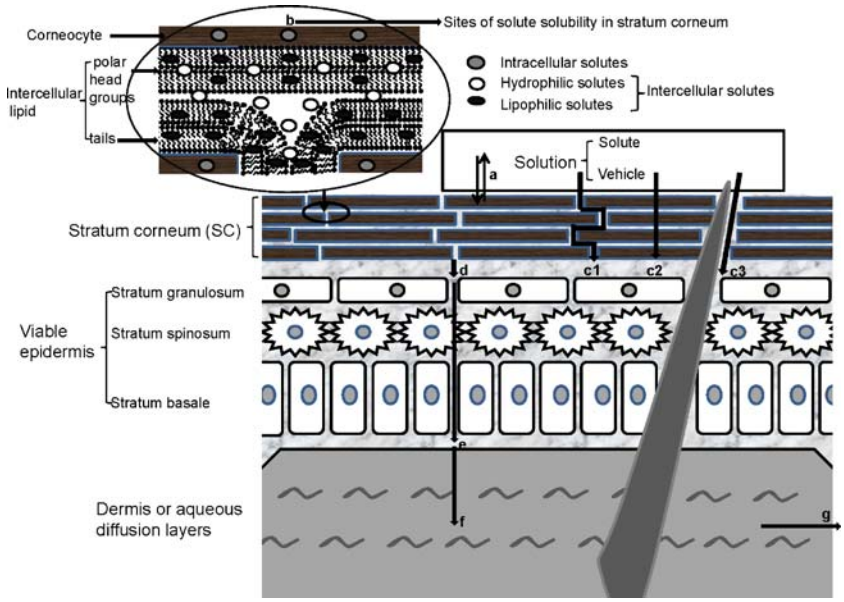

Fig. 1. A schematic depiction of a typical skin membrane and the diffusion process involved in solute penetration through the skin. (**a**) Partitioning between vehicle and stratum coneum. (**b**) Sites of solute solubility in the stratum corneum. (**c**) Possible pathways of solute penetration through stratum coneum (c1-transcellular route, c2-intercellular route, c3-follicular route). (**d**) Partitioning across the stratum corneum–viable epidermis interface. (**e**) Barrier resistance by the viable epidermis. (**f**) Barrier resistance by the dermis or aqueous diffusion layers in *in vitro* study. (**g**) Clearance from the dermis or aqueous diffusion layers.

donor. This partition coefficient can be defined as the ratio of solute concentrations in the stratum corneum (C_{SC}) and in the vehicle (C_v), *i.e.:*

$$K_{SC} = C_{SC}/C_v \tag{4}$$

The expression for Eq. 1 approaches a linear steady-state $Q_{SS}(t)$ – in that limit, the final summation term in Eq. 1 becomes negligible:

$$Q_{SS}(t) = J_{SS}A\left(t - t_{lag}\right) \tag{5}$$

The permeability coefficient k_p is the coefficient of proportionality between the steady-state flux J_{SS} and the aqueous donor concentration C_v:

$$k_p = J_{SS}/C_v \tag{6}$$

When using saturated solutions, $C_v = S_{aq}$, and here K_{sc} can be estimated by:

$$K_{SC} = S_{SC}/S_{aq} \tag{7}$$

where S_{SC} is the solubility of solute in the stratum corneum, and the J_{max} corresponds to the J_{SS} for a saturated donor concentration (S_{aq}):

$$J_{\max} = k_p S_{aq} = S_{SC}D/h \tag{8}$$

which combined with Eq. 3 gives:

$$D = 6t_{lag}\left(\frac{J_{\max}}{S_{SC}}\right)^2. \tag{9}$$

In the particular cases of a limited volume or finite applied solution and/or a limited volume or finite receptor, assumed conditions of constant donor and zero receptor concentrations are approximate only. However, the effects of finite conditions on the steady-state flux are relatively easily corrected using Fick's first law, as follows:

$$J = \frac{DS_{SC}}{h}\left(\frac{C_v}{S_{aq}} - \frac{C_r}{S_r}\right) = J_{\max}(F_d - F_r), \tag{10}$$

$$F_d = C_v/S_{aq}, \tag{11}$$

$$F_r = C_r/S_r; \tag{12}$$

where S_r is the solute solubility in the receptor solution.

Lipophilicity of a solute is usually measured as the solute's octanol-water partition coefficient P, and is defined as the ratio of the equilibrium concentrations of solute in octanol and in water (or, for saturated solutions, as the ratio of the solubilities in octanol and in water). Previous membrane permeation studies have shown that log J_{max} can be related with log P by a parabolic relationship to recognise that solutes with high log P poorly dissolve in the aqueous phase below the lipid membrane (29–34,40,41):

$$\log(J_{\max}) = a + b\log P + c(\log P)^2, \tag{13}$$

or a bilinear relationship to describe drug partitioning between a series of aqueous and lipid compartments (42, 43):

$$\log(J_{\max}) = a + b\log P + c\log(dP + 1). \quad (14)$$

MATERIALS AND METHODS

Test Solutes

Methyl paraben (99%), β-naphthol (99%), methyl salicylate (99%), chlorocresol (99%), thymol (98%), phosphate buffered saline (pH 7.4, PBS) sachets, HPLC grade acetonitrile and AR grade ethanol was purchased from Sigma-Aldrich (Castle Hill, NSW, Australia). 4-Propoxyphenol, iso-thymol, o-t-butylphenol, chloroxylenol, and p-n-butylphenol were purchased from Novachem Pty Ltd (Collingwood, VIC, Australia) as pure (>99%) substances.

Determination of S_{aq} and P

S_{aq} was determined by adding an excess amount of each solute to 5 mL of deionised and distilled water (5 replicates for each solute). The samples were continuously agitated by magnetic stirrer bars and incubated in a water bath at 32°C for 72 h. Serial timed samples were subsequently centrifuged at 14,000 rpm for 5 min at 32°C. The supernatant was immediately taken and diluted for high-performance liquid chromatography (HPLC) assay. Solubility in receptor phase was measured with the same method above. P was determined by the classic shake-flask method described previously (44–46), and expressed in logarithmic (base 10) form as log P. The method involved dissolving accurately weighed compounds in water-saturated octanol, adding water and monitoring changes in water concentrations of compounds with intensive shaking time until equilibration was reached (usually within 4 h). Known volumes of the octanol and water phases were analysed by HPLC for each solute.

Human Skin Preparation

Human epidermal membranes were prepared from abdominal full thickness skin using heat separation (47). The skin was provided by one female donor (aged 44), following an elective surgical procedure, with ethical approval granted by the Princess Alexandra Hospital Human Research Ethics Committee and Wesley Hospital Ethics Committee. The epidermal membranes were stored at −20ºC and used within 3 months.

Determination of S_{SC}

For partitioning studies, stratum corneum was prepared from epidermal sheets by trypsin digestion (47), then stored frozen at −20ºC until use. Circles of thawed stratum corneum (4 replicates for each compound) were weighed before hydration to ensure a stable weight. They were then supported on a silver wire mesh and equilibrated in a saturated aqueous solution (1 mL) of each test solute at 32ºC in screw-topped glass vials for 24 h, according to established methods (48,49). At the end of the incubation period, the stratum corneum was removed and blotted dry. To extract the solutes, the stratum corneum circles were suspended in 1 mL of 70% ethanol/water in an Eppendorf tube for another 24 h, at the same temperature used for equilibration (32ºC). The efficiency of recovery of known amounts of all nine of the solutes by this technique was between 96–98%, with methyl salicylate being 94%. The solute concentration in the equilibrating solution was measured after the 24 h period and a reduction of <1% was seen in all cases, indicating that the solution remained saturated. The S_{SC} was determined from the amount of the recovered phenolic compound in the extraction fluid, measured by HPLC, divided by the weight of the stratum corneum.

Human Skin Flux Studies

The epidermal membranes were cut into discs and mounted, stratum corneum side uppermost, in horizontal glass Franz-type static diffusion cells (exposed surface area approx 1.33 cm^2, 4–5 replicates for each solute). To assess the integrity of the epidermal membrane, the donor and receptor chambers were filled with PBS buffer and the cells were equilibrated for 30 min before transepidermal electrical resistance was measured with a standard multimeter. Skin samples with resistance less than 50 $k\Omega \cdot cm^{-2}$ were considered damaged and were discarded (50). Donor and receptor chambers were then emptied and the receptor chambers filled with approx. 3.5 mL PBS buffer containing 10% ethanol. Diffusion cells were placed in a water bath at 35ºC, in order to maintain a membrane surface temperature of approximately 32ºC (by thermocouple measurement, mean 32.1ºC), and the receptor chambers were constantly stirred with magnetic fleas.

The initial donor concentrations used for each compound were a saturated solution in water and a 10% dilution of this saturated solution. When a discrepancy between observed maximum flux ($J_{max,observed}$) and maximum fluxes estimated from the dilute solution ($J_{max,estimated}$) occurred, a third solution was used, at a 30% dilution of the saturated solution concentration, in order to investigate whether any skin damage had been caused by high solute concentrations. At t=0, an "infinite" dose (3±0.3 mL) of test solution was added to completely fill the donor chamber, which was covered with a glass cover slip to minimize evaporation from the donor phase. Samples of receptor phase (200 μL) were then removed at regular time points over the next 7 h and replaced with same amount of fresh 10% ethanol in PBS buffer. After the last sampling time point, the donor solution was collected, and the total volume measured. Drug concentrations in receptor and donor samples were determined by HPLC.

Sample Analysis

Drug levels in solutions and extraction samples were analyzed using a HPLC system consisting of a Shimadzu SIL-6B® SCL-10A VP system controller, a SPD-10AV UV-VIS detector, LC-10AD a pump and an autoinjector. The mobile phases were all pumped through the system at a flow rate of 1 mL/min. The column used was an Agilent ZORBAX Eclipse Plus-C8 (3.5 um, 150 × 4.6 mm). The UV wavelengths for different compounds are listed in Table I.

Table I. Molecules Chosen for this Study: Relevant Physicochemical and HPLC Parameters

S1

S2

Phenolic Compound	Structure (R1,2,3,4,5 for S1)	MW [a]	MP [b] (°C)	pKa [a]	log *P* [a]	MV [a] cm^3/mol	*PSA* [a] A^2	$\alpha/\beta/\pi$	Wavelength [c] (nm)
methyl paraben	R3= COOMe	152	131	8.30*	1.86	125.7	46.5	0.69/0.45/1.37	214
4-propoxyphenol	R3= OPr-n	152	55	10.34†	2.37	144.8	29.5	0.57/0.52/1.17	276
methyl salicylate	R1= COOMe	152	–8	9.76†	2.23	125.7	46.5	0.01/0.48/0.82	276
β-naphthol	S2	144	123	9.57*	2.71	121.9	20.2	0.61/0.40/1.08	214
chlorocresol	R2= Me, R3= Cl	143	67	9.63†	2.89	116.0	20.2	0.65/0.22/1.02	276
iso-thymol	R2= Pr-i, R5= Me	150	1	10.83†	3.28	154.2	20.2	0.54/0.36/0.81	276
thymol	R1= Pr-i, R4= Me	150	52	10.59†	3.28	154.2	20.2	0.52/0.44/0.79	276
o-t-butylphenol	R1=Bu-t	150	–6.8	11.34†	3.17	154.5	20.2	0.52/0.40/0.92	278
chloroxylenol	R2, R4= Me, R3=Cl	156	115	9.76†	3.35	132.3	20.2	0.64/0.21/0.96	280
p-n-butylphenol	R3= Bu-n	150	22	10.11†	3.54	153.6	20.2	0.55/0.37/0.88	278

MW–molecular weight; MP–melting point; MV–molar volume; PSA–polar surface area; α/β-hydrogen-bond acidity/basicity; π-dipolarity/polarisability of solute
[a] theoretically predicted data from SciFinder Scholar 2006; [b] experimental data from SciFinder Scholar 2006; [c] wavelength for HPLC detection of sample analysis; * -pH of donor (6.3–6.4); † -pH of donor (6.6–6.8)

Data Analysis

From the initial solubility studies, we obtained estimates for solute S_{aq}, S_{SC} and solute *P*. The K_{SC} was then estimated via Eq. 7. We obtained the values of J_{max}, k_p and *D* from the penetration studies. The steady-state flux J_{SS} and lag time t_{lag} of a solute were determined by nonlinear regression of the full analytical solution (Eq. 1) in the Laplace domain (39), using the program Scientist 3.0 (Micromath Research, St Louis, USA). Values of J_{max} were either steady-state fluxes observed for saturated solutions ($J_{max,observed}$), or steady-state fluxes observed for sub-saturated solutions divided by the ratio C_v/S_{aq} , *i.e.:*

$$J_{\max,estimated} = J_{SS} \cdot S_{aq}/C_v \tag{15}$$

The k_p was then calculated using Eq. 6, and *D* using Eq. 9.

All data were compared with values obtained from the literature, including previous phenolic compound epidermal k_p and K_{SC} reported by Roberts (9). Linear or nonlinear regressions (using the parabolic or bilinear models) of penetration or solubility data with log *P* were also performed using Scientist 3.0.

RESULTS

Table I shows HPLC detector wavelengths and physicochemical parameters obtained from the literature for the 10 phenolic solutes used in the present study. Whilst the solutes chosen in this study have a molecular weight range of 150±7, it is noted that the range in molar volume is somewhat wider (138.2±16.3). The range of log *P* (from 1.95 to 3.52) values indicates a variation over two orders of magnitude in the octanol-water partitioning of the chosen compounds. In addition, as the *pKa* values of the phenols are more than two *pH* units above the *pH* of the solutions used, each of the compounds studied was essentially all in the unionised form (>99%). Huq *et al.* (15) reported that the k_p of phenolic compounds with a *pKa* of 7.15 or less varied with the *pH* of the donor aqueous solution, due to partial ionisation; but our choice of phenolic compounds and solution pH circumvents this problem. Furthermore, the polar surface area (*PSA*) from SciFinder Scholar 2006, as well as the solvatochromic parameters, solute hydrogen-bond acidity/ basicity (α/β), and dipolarity/polarisability of solute (π) (51–53), are included to illustrate the H-bonding abilities of the compounds.

Table II shows the observed values of S_{aq} and S_{SC}, as well as estimated K_{SC} and log *P* values for the phenolic compounds. The experimental log *P* values in Table II (from our results) are generally similar to the theoretically predicted log *P* values from SciFinder Scholar 2006. Significant deviations were evident, however, for experimental (at 32ºC) and predicted S_{aq} values (Table II). Experimental S_{aq} determined at lower temperatures (at 25ºC and 20ºC) by other authors appear to be consistent with the experimental values reported here (Table II).

The dependence of the accumulated amount of solute in the receptor phase, as a function of time, was consistent with the Fick's law model. Table III shows estimates for the parameters describing human epidermal solute fluxes. For all solutes, other than 4-propoxyphenol and chlorocresol, J_{max}

Table II. Solubilities of Phenolic Solutes in Water from the Literature, and from our Work (S_{aq}); Solubilities in Stratum Corneum from our Work (S_{sc}); Estimated Values for Stratum Corneum-Water Partition Coefficients (K_{SC}); and Experimental Values for P (given as log P). Values Obtained in this Work are Expressed as Mean±SD

Phenolic Compound	S_{aq} (25°C) [a] (mg/L)	S_{aq} [b] (mg/L)	S_{aq} (32°C) [c] (mg/L)	S_{SC} (24h) [c] (μg/mg)	K_{SC} [c] (mL/g)	log P [c]
methyl paraben	64000	2500 [d]	2123.1±58.2	23.2±3.2	10.9±1.8	1.95±0.03
4-propoxyphenol	3700	2890 [d]	3435.7±82.5	57.9±4.4	16.9±1.7	2.34±0.06
methyl salicylate	7800	700 [e]	1470.2±76.7	41.8.±6.9	28.5±6.2	2.48±0.05
β-naphthol	500	755 [d]	1191.7±54.4	46.0±6.2	38.6±7.0	2.72±0.02
chlorocresol	4100	3830 [d]	4905.9±104.8	232.2±18.3	47.3±4.7	3.07±0.04
iso-thymol	840	1250 [d]	1325.0±67.2	79.4±5.6	59.9±7.3	3.27±0.03
thymol	840	900 [f]	928.4±23.5	57.3±6.4	61.7±8.5	3.31±0.02
o-t-butylphenol	1200	700 [d]	628.1±52.1	41.3±3.5	65.7±11.0	3.33±0.03
chloroxylenol	1200	250 [f]	456.4±22.9	31.1±3.2	68.1±10.4	3.38±0.02
p-n-butylphenol	690	220 [d]	248.5±30.8	21.5±2.6	86.5±21.2	3.52±0.03

[a] theoretically predicted data from SciFinder Scholar 2006;
[b] values from Environmental Science Centre PhysProp online database;
[c] obtained in this work, expressed as (mean±SD);
[d] 25ºC; [e] 30ºC; [f] 20ºC

observed with saturated aqueous solutions were similar to those estimated from the 10% and 30% dilutions. The logarithm of $J_{max,observed}$ values for 4-propoxyphenol and chlorocresol were estimated to be 24% and 17% greater than the predicted values from $J_{max,estimated}$, respectively.

In Fig. 2 we show the variation of estimates of J_{max} with log P values, and compare with the variation of estimates of S_{SC} with log P. It is apparent that the variation of log S_{SC} with experimental log P (Fig. 2D) has a similar nature to that seen for the variation of log J_{max} with log P, for both experimental (Fig. 2A) and theoretically predicted (Fig. 2B) log P values. In all cases, we observe a convex relationship with a maximum at log P between 2.7 and 3.1. Fig. 2C shows that the plots of $J_{max,estimated}$ from a 10% dilution *versus* experimental log P are better described by a bilinear than a parabolic relationship (n = 10):
Bilinear:

$$\log J_{\max} = -2.1(\pm 0.2) + 1.7(\pm 0.1)\log P - 21.6(\pm 0.5) \times \log\left[10^{-4}\left(\pm 2.6 \cdot 10^{-6}\right) \cdot 10^{\log P} + 1\right] \quad r^2 = 0.86$$

Parabolic:

$$\log J_{\max} = -7.2(\pm 2.0) + 6.5(\pm 1.5)\log P - 1.2(\pm 0.3) \times (\log P)^2 \quad r^2 = 0.74$$

By contrast, we observe in Table III that the values of t_{lag} for the phenols are relatively constant, suggesting a low dependence of diffusivity on lipophilicity; further to this, the variation of log D with log P (Fig. 3A) suggests that, for solutes of similar size, diffusivity of solutes in the stratum corneum is invariant with log P. β-naphthol appears to have a lower S_{SC} and higher D than the other phenolic compounds studied here. A further plot (Fig. 2E) demonstrates a good linear relationship between the log J_{max} and log S_{SC} (r^2=0.88).

Table III also shows the solute concentration remaining in the donor, given as a fraction of donor phase solubility (F_d) and the concentration recovered in the receptor phase as a fraction of the receptor phase solubility (F_r) at the end of the study for each solute (calculated via Eqs. 11, 12). It is apparent that the depletion in the donor phase is not overly significant and that receptor concentrations are much lower than the receptor phase solubility. Apart from the chlorocresol case, where C_v=S_{aq} and F_r=0.13, all solutes had F_r values below 0.1, consistent with the recommendation that the effective concentration in the receptor for these compounds should be less than one-tenth the solubility for the solute in the receptor (54). For donor solutions with concentrations at 10% or 30% solubility, F_r is proportionately smaller.

A lower than expected J_{max} would also arise if the donor concentration decreased throughout the study due to evaporation, binding or depletion (as can be the case for finite donors). In this study, the maximum decrease in C_v over the study occurred for chlorocresol in saturated solution, with F_d =0.76. Hence, the log value of flux at the last sampling time would be log J_{max} – log (F_d -F_r) ≈ log J_{max} + 0.2. Note, however, that this correction would be less at earlier sampling times, and it is reasonable to assume that the correction to the regression slope would be 3 to 4 times smaller than this, giving a maximum correction of approximately 0.05. By contrast, the smallest correction to the last sampling time (in the case of methyl paraben) would be –log (0.9) ≈ 0.05. Thus, in the worst case, the errors induced by the finite donor and receptor would be of the same order as the experimental error – for other cases these errors would be much less significant.

Relationships between log K_{SC} (mL/g) and log P (Fig. 3B) and between log k_p (cm/min) and log P (Fig. 3C) were also examined. It is apparent that the data obtained here are similar to those obtained for similar molecular weight phenols by Roberts (9) at 32ºC using side by side diffusion cells. Both figures demonstrate good linear relationships (n=10):for log K_{SC} we obtain:

$$\log K_{SC} = 0.54(\pm 0.03) \cdot \log P + 0.03(\pm 0.10) \quad r^2 = 0.97,$$

while for log k_p we obtain:

$$\log k_p = 0.56(\pm 0.10) \cdot \log P + 0.20(\pm 0.29) \quad r^2 = 0.81.$$

Table III. Permeation Data for Phenolic Solutes Through Stratum Corneum: Fluxes Estimated from Dilute Solutions (log $J_{max,\ estimated}$) and Maximum Fluxes Observed from Saturated Solutions (log $J_{max,\ estimated}$); Permeability Coefficients (k_p); and Log of Diffusion Coefficient (D); Ratio for Observed Highest Concentration and Solubility in the Receptor (F_r); Ratio for Final Concentration of Donor and Initial Concentration of Donor (F_d). Values Obtained in this Work are Expressed as Mean±SD

Phenolic Compound	log P (experimental)	log ($J_{max,\ observed}$) [a] (μg/cm²/h)	log ($J_{max,\ estimated}$) (μg/cm²/h)	k_p [b] (10^4cm/min)	t_{lag} [b] (min)	log($D{\cdot}10^5$cm²/h) [b]	F_r [a]	F_d [a]
methyl paraben	1.95±0.03	1.31±0.04	1.25±0.04[b]	1.4±0.2	21±3	1.09±0.08	0.01	0.89
4-propoxyphenol	2.34±0.06	2.26±0.05	1.71±0.06[b]; 1.68±0.06[c]	2.5±0.4	16±5	1.10±0.11	0.06	0.83
methyl salicylate	2.48±0.05	1.68±0.04	1.72±0.05[b]	6.0±1.0	20±4	1.50±0.10	0.07	0.78
β-naphthol	2.72±0.02	1.92±0.05	1.87±0.04[b]	10.5±1.4	15±6	1.60±0.14	0.08	0.80
chlorocresol	3.07±0.04	2.70±0.06	2.25±0.05[b]; 2.21±0.07[c]	6.0±0.8	17±4	1.00±0.09	0.13	0.76
iso-thymol	3.27±0.03	1.92±0.05	1.87±0.06[b]	9.3±1.8	16±3	1.15±0.09	0.07	0.79
thymol	3.31±0.02	1.79±0.07	1.76±0.05[b]	10.2±1.4	18±3	1.25±0.09	0.07	0.81
o-t-butylphenol	3.33±0.03	1.71±0.06	1.67±0.07[b]	12.4±3.0	17±4	1.34±0.10	0.06	0.84
chloroxylenol	3.38±0.02	1.52±0.07	1.57±0.04[b]	13.4±1.9	15±5	1.32±0.11	0.07	0.77
p-n-butylphenol	3.52±0.03	1.40±0.05	1.28±0.06[b]	12.8±3.4	18±4	1.15±0.10	0.06	0.84

[a] Values calculated from saturated solution; [b] estimated from a 10% dilution of a saturated solution; [c] estimated from observed steady-state flux found with a 30% dilution of a saturated solution

The phenols used here, other than methyl salicylate, had similar total hydrogen-bond (α+β) values (range 0.85 to 1.14). In addition, attempted linear regression for log J_{max} with *PSA* and solvatochromic parameters α, β, $(\alpha+\beta)$ and π yielded correlations that were not statistically significant ($r^2 < 0.2, p > 0.05$) and had a random distribution of residuals, which suggests that H-bonding is not a key determinant for the convex relationship found between log J_{max} and log P (Fig. 2C).

5. DISCUSSION

The important finding in this work is that when solutes of a similar size (i.e. similar molecular weight) and hydrogen bonding capacity permeate the skin, there is a convex relationship between log J_{max} and log P that is matched by the relationship between log S_{SC} and log P. In particular, we note that the decrease in J_{max} with increasing lipophilicity is a real phenomenon, not due solely to the effects of increasing molecular size that have confounded the conclusions of previous studies.

In contrast to the strong dependence of J_{max} on log P, the estimated diffusivity D and lag time t_{lag} appear to be independent of log P. Thus we observe that molecules with similar molecular weights (or molar volume) and hydrogen bonding, but various log P, exhibit similar diffusivities, but various maximum fluxes. This result suggests a model for J_{max} where the diffusion contribution (see Eq. 8) is determined by molecular weight and hydrogen bonding, while the solubility contribution is relatively independent of these parameters. Such a model is supported by the known strong dependence of J_{max} on molecular weight and molar volume for aqueous solutions (3) and on hydrogen bonding (8,10,11), and experimental data indicating that S_{SC} is relatively independent of these parameters (55). It is consistent with t_{lag} being invariant with log P for solutes of similar size when the size dependence for J_{max} is so significant (3). In the present work, the hydrogen bond present was a single phenolic group. Other studies have shown that t_{lag} (and hence, diffusivity) is also greatly affected by the number and type of H-bonding groups on the solute (6,8). Molar volume may be a more representative measure of size than molecular weight, and dependencies of J_{max} on molar volume have been given by Hinz *et al.* (32) and Magnusson *et al.* (3). Adopting a molar volume-based model instead of a molecular weight-based model leads to a possible correction of up to 20% (in the case of chlorocresol). However, such a correction does not affect the relationship with log P, and therefore does not alter our conclusions about the mechanisms involved.

Validation of J_{max} values obtained from saturated solutions, using estimates ($J_{max,estimated}$) from more dilute solutions is necessary to ensure that solute effects on the skin, or nonlinear solute-vehicle interactions, do not confound the J_{max}–lipophilicity relationship. In this work, saturated solutions of 4-propoxyphenol and chlorocresol led to a small increase in J_{max} over that estimated from 10% or 30% solutions. We had previously suggested a threshold concentration of ~0.5% for phenolic compounds in water, above which damage could occur (6). At saturation, chlorocresol just reaches this limit (0.49%) and propoxyphenol (0.34%) is close to it. Consistent with the present findings, Huq *et al.* (15) showed that the J_{max} values obtained directly from

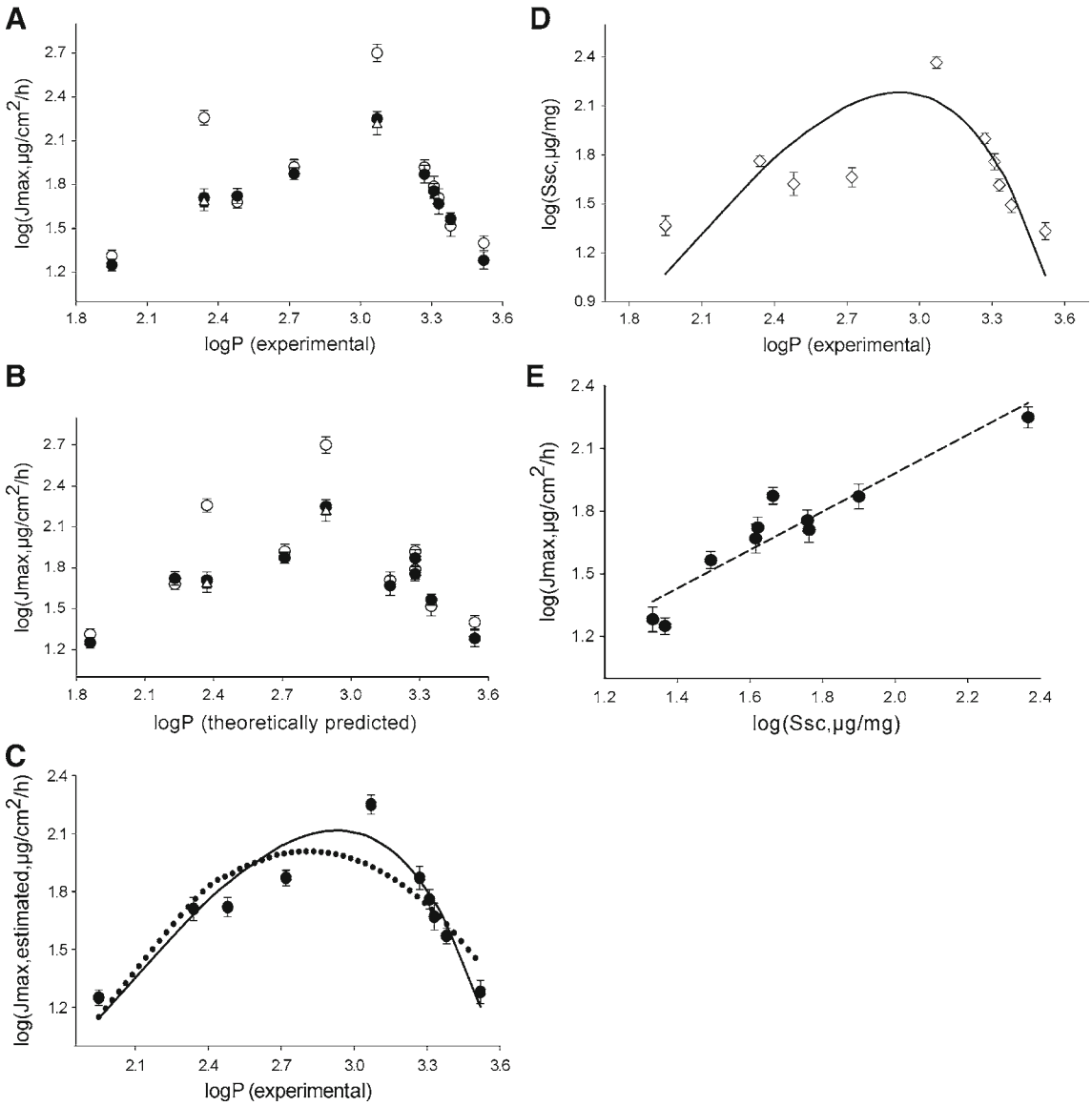

Fig. 2. Dependence of maximum flux J_{max} and stratum corneum solubility S_{SC} on log P for penetration of phenolic compounds through excised human epidermal membranes using Franz cells (mean ± SD). Filled circles are values of log $J_{max,\ estimated}$ from 10% dilution of a saturated solution; open triangles are values of log $J_{max,\ estimated}$ from 30% dilution of a saturated solution; open circles are values of log $J_{max,\ observed}$ from a saturated solution. Open diamonds are values of log S_{SC} obtained in this study at 32°C using desorption method (mean ± SD). (**A**) Log J_{max} *versus* experimentally determined estimates of log P. (**B**) Log J_{max} *versus* theoretically predicted log P values from SciFinder Scholar. (**C**) Bilinear (solid line) and parabolic (dashed line) model fits for log $J_{max,estimated}$ (10% dilution) *versus* experimental log P. (**D**) Bilinear relationship between log S_{SC} and experimental log P. (**E**) Linear relationship between log J_{max} and log S_{SC} (r^2=0.88).

saturated chlorocresol doubled the estimated value for J_{max}. Higher concentrations may also lead to a decrease in flux, as has been shown for pentanol in arachis oil (56), due to dehydration of the skin and association in the oil (57).

The convex relationship we observe between log J_{max} and log P is consistent with a number of earlier studies *in vitro* (29,30,32), for man *in vivo* (33,34), and in rat skin (31,40). Maximum fluxes through rat skin have been shown to occur with log P values of around 3 (40), and Lien and Tong (4) derived a maximum log P range of 2.5 to 3.6 on the analysis of the structure penetration relationships for a number of solutes through skin. The relationship between log $J_{max,estimated}$ and log P appears to be more closely modelled as bilinear rather than parabolic (Fig. 2C) and is consistent with the findings by Hinz *et al.* (32) for phenolic compound transport through hairless mouse skin. This result has been attributed to an underlying transport process where the solute partitions into a series of aqueous and lipid compartments (42,43), rather than partitioning from a lipid membrane to a single aqueous phase. In the present situation, the intercellular lipid polar head groups region and corneocyte matrix provide a polar environment, whereas the lipophilic intercellular lipid tails provide a lipid environment and transport occurs through there in series (Fig. 1).

Given that the compounds used in this study have an S_{aq} greater than 0.025%, we do not expect significant rate-

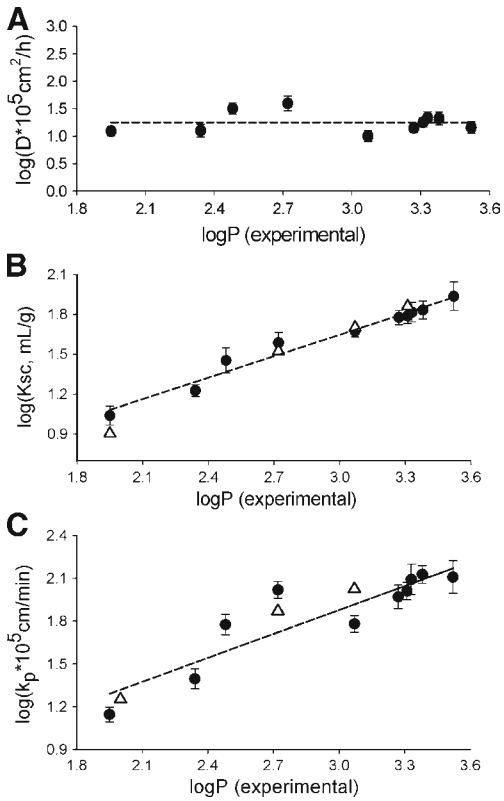

Fig. 3. Variation of D, K_{SC} and k_p, with experimental log P. Filled circles indicate estimates obtained from this study. (**A**) Estimates of log D (filled circles); the dashed line is the linear fit indicating the small variation in log D observed in this study (r^2=9E-07). (**B**) Estimates of log K_{SC}, (filled circles) derived from the ratio of S_{SC} and S_{aq}, with linear regression (r^2=0.97). Open triangles show values for compounds with similar molecular weight obtained by Roberts (9) at 32°C using side by side diffusion cells. (**C**) Estimates of log k_p, (filled circles) with linear regression (r^2=0.81). Open triangles show values for compounds with similar molecular weight obtained by Roberts (9) at 32°C using side by side diffusion cells.

limiting partitioning across the stratum corneum–viable epidermis interface (32) or epidermal-aqueous diffusion boundary interface (6), even for the more lipophilic and less water soluble solutes in this study. Such a limitation corresponds to non-sink receptor conditions, when the solute has significant thermodynamic activity at low concentrations (significant F_r). By avoiding solutes with a low S_{aq}, such a condition should not arise. Furthermore, the 10% ethanol receptor was used not only to facilitate sink conditions but also to mimic the known binding of phenols to extracellular skin components such as collagen (58) and to blood proteins (59,60).

A number of authors, including ourselves, had previously proposed that the curvature in permeability with increasing lipophilicity was due to a change in the permeation rate-limiting barrier from the stratum corneum to either the viable epidermis, dermis or, in *in vitro* studies, to the unstirred aqueous diffusion layer (6,13,32,61). Support for this hypothesis is also provided by the work of Huq *et al.* (15), who showed that the k_p values for the more lipophilic phenols, including chlorocresol, applied to mouse skin sections from which the stratum corneum had been removed by adhesive tape stripping were less than double those for skin with the stratum corneum intact. In contrast, Anderson and Raykar (19) examined the penetration of methyl substituted p-cresols through untreated and delipidized stratum corneum at 37ºC and found that delipidization dramatically increased k_p. They found that the highest delipidized k_p was comparable to a solute diffusivity of 10^{-5} cm^2s^{-1} and an aqueous barrier layer thickness of 300μm. Using the suggested viable epidermal k_p of about $10^{-6}m{\cdot}s^{-1}$ and its contribution to the overall skin permeability (21), the estimated log P at which the viable epidermis will contribute to epidermal k_p is 4.3. Potts and Guy (21), in drawing conclusions about the lipophilicity and size dependency of the switch to an epidermal k_p-limiting process, had commented that experiments validating their hypothesis had not yet been performed. The present data appears to provide validation of the Potts and Guy hypothesis – as log P values approach 4.3, our results indicate that stratum corneum permeation will be of a similar order of magnitude to that through the viable epidermis.

The possible dependence of J_{max} on S_{SC} (in particular, the variation in diffusivity) has been alluded to by a number of authors (35,36,62). In addition, Kasting *et al.* suggested that log $J_{max,}$ could be related to the solubility of solutes and their molecular weight (63). In our modification of this relationship (64) using the Potts-Guy (21) relationship for log k_p *versus* log P and S_{aq} to estimate J_{max}, we concluded that the slope of the relationship between log J_{max} and solubility of the solute in octanol should be 0.71 (64). We have previously suggested that implicit in this lower slope is a polarity for the stratum corneum that is less than octanol – probably more like butanol (6), implying that the maximum log P for partitioning into stratum corneum is ~ 2.24 (64). The actual log P for maximum transport of phenolic compounds observed here (2.7 to 3.1) is somewhat higher and closer to that assumed by Kasting and colleagues (63). Interestingly, the log P for maximum transport for phenolic compounds has previously been estimated to be ~2.23 in excised mouse skin (32), and ~2.5 (33) or ~2.7 (34) in human skin *in vivo*. The discrepancy in the apparent log P for maximal transport could reflect, in part, the solvent in which the phenols are applied. It has been suggested that solute penetration through the stratum corneum can occur through both the intercellular and transcellular route (23) and that methyl substituted *p*-cresols mainly partition into the protein domain of the stratum corneum (45). However, our recent multiphoton imaging studies on the transport of β-naphthol in the stratum corneum suggests that β-naphthol mainly partitions into the intercellular lipids when applied as an aqueous solution but is taken up into corneocytes when an organic solvent is present (27). In contrast to the aqueous solutions used in this work, Hinz *et al.* (32) and Yano *et al.* (34), applied solutes in acetone, which formed solid deposits when the acetone evaporated. Hence, one explanation for the lower log P for J_{max} in those studies relative to the present study is a greater partitioning of solutes into the corneocyte protein domain when solutes were applied in acetone than when applied in water, as studied in this work.

The linear variations of log K_{SC} and log k_p with log P (Fig. 3B and C) are similar to those we obtained previously for phenolic solutes (6, 55, 65), with consistent slopes, and the

estimated diffusivity for the similar size phenols in the present study is comparable (Fig. 3A). The slope of 0.6 found between log k_p and log P (Fig. 3C) is similar to the slope of 0.7 reported by Potts and Guy (21). A linear relationship between log k_p and log P has also been reported for mouse skin and silicone rubber membranes (66). Further, in the present study, the hydrogen bonding properties of the solutes did not appear to be significant determinants for J_{max}. Hydrogen bonding has also been suggested as a determinant of epidermal penetration, with the numbers of hydrogen bonds (3,9), solvatochromic parameters (10,11,52) and *PSA* (67– 69) being used for epidermal and intestinal transport. The solutes used in present study essentially had a single -OH available for hydrogen bonding; whereas in our earlier work, some of the phenols had additional -OH and -NO_2 groups. The inclusion of such compounds would greatly increase the slope for log k_p *versus* log P or log K_{SC}, as these more polar compounds have a lower diffusivity. This effect may be expected to be most pronounced when there is a range of polar groups and may explain the higher slope of 3.6 for a log k_p *versus* log K_{SC} plot observed by Anderson and Raykar (19), compared to the slope of ~ 1 and the constant diffusivity with lipophilicity observed here. While in previous work we have attributed deviations from a linear log k_p–log P relationship for more lipophilic phenols to a change in the site of epidermal resistance (55), the present study would suggest a linear log k_p–log P solute structure-skin permeability model in which deviations are accounted for by variations in diffusivity induced by solute size or hydrogen bonding. These findings support earlier models of skin permeability in which skin k_p values were initially related to P and solute size (14,21) and later, in addition, the hydrogen bonding of solutes (8,10,11).

In conclusion, the present J_{max} *versus* log P results from saturated aqueous solutions through human epidermis are similar in shape to those obtained by Hinz *et al.* (32) for solvent deposited phenolic compounds through mouse skin. However, a key finding in the present work is that S_{SC} – and not a diffusional resistance by deeper tissues/aqueous boundary layers or an inability for a solute to partition into the receptor fluid or variation in solute size – is responsible for the parabolic behaviour observed for J_{max} for the phenolic compounds studied here. Furthermore, the decrease in J_{max} for increasing lipophilicity is observed for solutes with essentially the same molecular size. It is likely that for less water-soluble solutes, partition rate-limited permeation will add to the curvature in the parabolic shape observed. This work is consistent with an underlying model where lipophilicity is associated with partitioning effects, while molecular size and hydrogen bonding properties are associated with diffusive characteristics.

ACKNOWLEDGEMENTS

The authors thank the National Health and Medical Research Council of Australia, National“863”Project (No. 2003AA2Z347A) from P.R China and National Nature Science Fund (30630076) from P.R China for financial support for this work. O.G. Jepps thanks the Australian Research Council for financial support (APD Fellowship) during this work. We also thank Prof M.H. Abraham from Department of Chemistry, University College London, for providing the solvatochromic parameters for methyl salicylate.

REFERENCES

1. Barry BW. Novel mechanisms and devices to enable successful transdermal drug delivery. Eur J Pharm Sci. 2001;14:101–14. doi:10.1016/S0928-0987(01) 00167-1.
2. Higuchi T. Physical chemical analysis of percutaneous absorption process from creams and ointments. J Soc Cosmet Chem. 1960;11:85–97.
3. Magnusson BM, Anissimov YG, Cross SE, Roberts MS. Molecular size as the main determinant of solute maximum flux across the skin. J Invest Dermatol. 2004;122:993–9. doi:10.1111/j.0022-202X.2004.22413.x.
4. Lien EJ, Tong GL. Physicochemical properties and percutaneous absorption of drugs. J Soc Cosmet Chem. 1971;24:371–84.
5. Scheuplein RJ, Blank IH. Permeability of the skin. Physiol Rev. 1971;51:702–47.
6. Roberts MS, Anderson RA, Swarbrick J. Permeability of human epidermis to phenolic compounds. J Pharm Pharmacol. 1977;29:677–83.
7. Michaels AS, Chandrasekaran SK, Shaw JE. Drug permeation through human skin: theory and *in vitro* experimental measurement. AIChE Journal. 1975;21:985–96. doi:10.1002/aic.690210522.
8. du Plessis J, Pugh WJ, Judefeind A, Hadgraft J. Physico-chemical determinants of dermal drug delivery: effects of the number and substitution pattern of polar groups. Eur J Pharm Sci. 2002;16:107–12. doi:10.1016/S0928-0987(02) 00085-4.
9. Roberts MS. Percuteneous absorption of phenolic compounds. PhD Thesis University of Sydney;1976.
10. Pugh WJ, Roberts MS, Hadgraft J. Epidermal permeability—Penetrant structure relationships: 3. The effect of hydrogen bonding interactions and molecular size on diffusion across the stratum corneum. Int J Pharm. 1996;138:149–65. doi:10.1016/0378-5173(96)04533-4.
11. Potts RO, Guy RH. A predictive algorithm for skin permeability: the effects of molecular size and hydrogen bond activity. Pharm Res. 1995;12:1628–33. doi:10.1023/A:1016236932339.
12. Yotsuyanagi T, Higuchi WI. A two phase series model for the transport of steroids across the fully hydrated stratum corneum. J Pharm Pharmacol. 1972;24:934–41.
13. Bunge AL, Cleek RL. A new method for estimating dermal absorption from chemical exposure: 2. Effect of molecular weight and octanol-water partitioning. Pharm Res. 1995;12:88–95. doi:10.1023/A:1016242821610.
14. Kasting GB, Smith RL, Cooper ER. Effect of lipid solubility and molecular size on percuatenous absorption. In: Shroot B, Schaefer H, editors. Skin Pharmacokinetics. Basel: Karger; 1987. p. 138–53.
15. Huq AS, Ho NF, Husari N, Flynn GL, Jetzer WE, Condie L Jr. Permeation of water contaminative phenols through hairless mouse skin. Arch Environ Contam Toxicol. 1986;15:557–66. doi:10.1007/BF01056570.
16. Cross SE, Roberts MS. Use of *in vitro* human skin membranes to model and predict the effect of changing blood flow on the flux and retention of topically applied solutes. J Pharm Sci. 2008;97:3442–50. doi:10.1002/jps.21253.
17. Elias PM, Friend DS. The permeability barrier in mammalian epidermis. J Cell Biol. 1975;65:180–91. doi:10.1083/jcb.65.1.180.
18. Albery WJ, Hadgraft J. Percutaneous absorption: *in vivo* experiments. J Pharm Pharmacol. 1979;31:140–7.
19. Anderson BD, Raykar PV. Solute structure-permeability relationships in human stratum corneum. J Invest Dermatol. 1989;93:280–6. doi:10.1111/1523-1747.ep12277592.
20. Guy RH, Potts RO. Structure-permeability relationships in percutaneous penetration. J Pharm Sci. 1992;81:603–4. doi:10.1002/jps.2600810629.
21. Potts RO, Guy RH. Predicting skin permeability. Pharm Res. 1992;9:663–9. doi:10.1023/A:1015810312465.

22. Pugh WJ, Hadgraft J. Ab initio prediction of human skin permeability coefficients. Int J Pharm. 1994;103:163–78. doi:10.1016/0378-5173(94)90097-3.
23. Wang TF, Kasting GB, Nitsche JM. A multiphase microscopic diffusion model for stratum corneum permeability. II. Estimation of physicochemical parameters, and application to a large permeability database. J Pharm Sci. 2007;96:3024–51. doi:10.1002/jps.20883.
24. Nitsche JM, Kasting GB. Biophysical models for skin transport and absorption. In: Roberts MS, Walters KA, editors. Dermal Absorption and Toxicity Assessment (2nd ed.). New York: Informa Healthcare USA; 2007. p. 251–69.
25. Yu B, Kim KH, So PT, Blankschtein D, Langer R. Visualization of oleic acid-induced transdermal diffusion pathways using two-photon fluorescence microscopy. J Invest Dermatol. 2003;120:448–55. doi:10.1046/j.1523-1747.2003.12061.x.
26. Hanson KM, Behne MJ, Barry NP, Mauro TM, Gratton E, Clegg RM. Two-photon fluorescence lifetime imaging of the skin stratum corneum pH gradient. Biophys J. 2002;83:1682–90. doi:10.1016/S0006-3495(02) 73936-2.
27. Winckle G, Anissimov YG, Cross SE, Wise G, Roberts MS. An integrated pharmacokinetic and imaging evaluation of vehicle effects on solute human epidermal flux and, retention characteristics. Pharm Res. 2008;25:158–66. doi:10.1007/s11095-007-9416-z.
28. Cross SE, Thompson MJ, Roberts MS. Transdermal penetration of vasoconstrictors–present understanding and assessment of the human epidermal flux and retention of free bases and ion-pairs. Pharm Res. 2003;20:270–4. doi:10.1023/A:1022235507186.
29. Cross SE, Magnusson BM, Winckle G, Anissimov Y, Roberts MS. Determination of the effect of lipophilicity on the *in vitro* permeability and tissue reservoir characteristics of topically applied solutes in human skin layers. J Invest Dermatol. 2003;120:759–64. doi:10.1046/j.1523-1747.2003.12131.x.
30. Magnusson BM, Cross SE, Winckle G, Roberts MS. Percutaneous absorption of steroids: determination of *in vitro* permeability and tissue reservoir characteristics in human skin layers. Skin Pharmacol Physiol. 2006;19:336–42. doi:10.1159/000095254.
31. Diez I, Colom H, Moreno J, Obach R, Peraire C, Domenech J. A comparative *in vitro* study of transdermal absorption of a series of calcium channel antagonists. J Pharm Sci. 1991;80:931–4. doi:10.1002/jps.2600801006.
32. Hinz RS, Lorence CR, Hodson CD, Hansch C, Hall LL, Guy RH. Percutaneous penetration of para-substituted phenols *in vitro*. Fundam Appl Toxicol. 1991;17:575–83. doi:10.1016/0272-0590(91) 90207-K.
33. Bucks D, Maibach HI. Occlusion dose not uniformly enhance penetration *in vivo*. In: Bronaugh RL, Maibach HI, editors. Percutaneous Absorption: drugs, cosmetics, mechanisms, methodology. Boca Raton: Taylor & Francis; 2005. p. 65–83.
34. Yano T, Nakagawa A, Tsuji M, Noda K. Skin permeability of various non-steroidal anti-inflammatory drugs in man. Life Sci. 1986;39:1043–50. doi:10.1016/0024-3205(86) 90195-5.
35. Liron Z, Cohen S. Percutaneous absorption of alkanoic acids II: Application of regular solution theory. J Pharm Sci. 1984;73:538–42. doi:10.1002/jps.2600730426.
36. Ando HY, Schultz TW, Schnaare RL, Sugita ET. Percutaneous absorption: a new physicochemical predictive model for maximum human *in vivo* penetration rates. J Pharm Sci. 1984;73:461–7. doi:10.1002/jps.2600730409.
37. Anissimov YG, Roberts MS. Diffusion modeling of percutaneous absorption kinetics. 1. Effects of flow rate, receptor sampling rate, and viable epidermal resistance for a constant donor concentration. J Pharm Sci. 1999;88:1201–9. doi:10.1021/js990053i.
38. Pellett MA, Roberts MS, Hadgraft J. Supersaturated solutions evaluated with an *in vitro* stratum corneum tape stripping technique. Int J Pharm. 1997;151:91–8. doi:10.1016/S0378-5173(97) 04897-7.
39. Roberts MS, Anissimov YG. Mathematical models in percutaneous absorption. In: Bronaugh RL, Maibach HI, editors. Percutaneous Absorption: drugs, cosmetics, mechanisms, methodology. Boca Raton: Taylor & Francis; 2005. p. 1–44.
40. Kim MK, Lee CH, Kim DD. Skin permeation of testosterone and its ester derivatives in rats. J Pharm Pharmacol. 2000;52:369–75. doi:10.1211/0022357001774101.
41. Hansch C, Clayton JM. Lipophilic character and biological activity of drugs. II. The parabolic case. J Pharm Sci. 1973;62:1–21. doi:10.1002/jps.2600620102.
42. Kubinyi H. Quantitative structure-activity relationships. IV. Nonlinear dependence of biological activity on hydrophobic character: a new model. Arzneimittelforschung. 1976;26:1991–7.
43. Kubinyi H. Drug partitioning: relationships between forward and reverse rate constants and partition coefficient. J Pharm Sci. 1978;67:262–3. doi:10.1002/jps.2600670237.
44. Leo A, Hansch C, Elkins D. Partition coefficients and their uses. Chem Rev. 1971;71:525–616. doi:10.1021/cr60274a001.
45. Anderson BD, Higuchi WI, Raykar PV. Heterogeneity effects on permeability-partition coefficient relationships in human stratum corneum. Pharm Res. 1988;5:566–73. doi:10.1023/A:1015989929342.
46. Takacs-Novak K, Avdeef A. Interlaboratory study of log P determination by shake-flask and potentiometric methods. J Pharm Biomed Anal. 1996;14:1405–13. doi:10.1016/0731-7085(96) 01773-6.
47. Kligman AM, Christophers E. Preparation of isolated sheets of human stratum corneum. Arch Dermatol. 1963;88:702–5.
48. Anderson RA, Triggs EJ, Roberts MS. The percutaneous absorption of phenolic compounds. 3. Evaluation of permeability through human stratum corneum using a desorption technique. Aust J Pharm Sci. 1976;5:107–10.
49. Roberts MS, Triggs EJ, Anderson RA. Permeability of solutes through biological membranes measured by a desorption technique. Nature. 1975;257:225–7. doi:10.1038/257225a0.
50. Mitragotri S. *In situ* determination of partition and diffusion coefficients in the lipid bilayers of stratum corneum. Pharm Res. 2000;17:1026–9. doi:10.1023/A:1007547809430.
51. Abraham MH. Scales of solute hydrogen-bonding-their construction and application to physicochemical and biochemical processes. Chem Soc Rev. 1993;22:73–83. doi:10.1039/cs9932200073.
52. Abraham MH, Chadha HS, Mitchell RC. The factors that influence skin penetration of solutes. J Pharm Pharmacol. 1995;47:8–16.
53. Mintz C, Acree WE, Abraham MH. Correlation of minimum inhibitory concentrations toward oral bacterial growth based on the Abraham model. QSAR Comb Sci. 2006;25:912–20. doi:10.1002/qsar.200630011.
54. Brain KR, Waters KA, Watkinson AC. Investigation of skin permeation *in vitro*. In: Roberts MS, Walters KA, editors. Dermal Absorption and Toxicity Assessment. New York: Marcel Dekker; 1998. p. 161–88.
55. Roberts MS, Anderson RA, Moore DE, Swarbrick J. The distribution of non-electrolytes between human stratum corneum and water. Aust J Pharm Sci. 1977;6:77–82.
56. Blank IH. Penetration of low-molecular-weight alcohols into skin. I. effect of concentration of alcohol and type of vehicle. J Invest Dermatol. 1964;43:415–20.
57. Roberts MS, Cross SE, Pellett MA. Skin transport. In: Walters KA, editor. Dermatological and Transdermal Formulations. New York: Marcel Dekker; 2002. p. 89–195.
58. Zhang Y, Lukacova V, Reindl K, Balaz S. Quantitative characterization of binding of small molecules to extracellular matrix. J Biochem Biophys Methods. 2006;67:107–22. doi:10.1016/j.jbbm.2006.01.007.
59. Ogata N, Shibata T. Binding of alkyl- and alkoxy-substituted simple phenolic compounds to human serum proteins. Res Commun Mol Pathol Pharmacol. 2000;107:167–73.
60. Mellick GD, Roberts MS. Structure-hepatic disposition relationships for phenolic compounds. Toxicol Appl Pharmacol. 1999;158:50–60. doi:10.1006/taap.1999.8682.
61. Guy RH, Hadgraft J. Physicochemical aspects of percutaneous penetration and its enhancement. Pharm Res. 1988;5:753–8. doi:10.1023/A:1015980516564.
62. Sloan KB, Koch SA, Siver KG, Flowers FP. Use of solubility parameters of drug and vehicle to predict flux through skin. J Invest Dermatol. 1986;87:244–52. doi:10.1111/1523-1747.ep12696635.
63. Kasting GB, Smith RL, Anderson BD. Prodrugs for dermal delivery: solubility, molecular size, and functional group effects. In: Sloan KB, editor. Produgs. New York: Marcel Dekker; 1992. p. 117–61.

64. Roberts MS, Walters KA. The relationship between structure and barrier function of skin. In: Roberts MS, Walters KA, editors. Dermal Absorption and Toxicity Assessment. New York: Marcel Dekker; 1998. p. 1–42.
65. Roberts MS, Anderson RA, Swarbrick J, Moore DE. The percutaneous absorption of phenolic compounds: the mechanism of diffusion across the stratum corneum. J Pharm Pharmacol. 1978;30:486–90.
66. Jetzer WE, Huq AS, Ho NF, Flynn GL, Duraiswamy N, Condie L Jr. Permeation of mouse skin and silicone rubber membranes by phenols: relationship to *in vitro* partitioning. J Pharm Sci. 1986;75:1098–103. doi:10.1002/jps.2600751116.
67. Stenberg P, Norinder U, Luthman K, Artursson P. Experimental and computational screening models for the prediction of intestinal drug absorption. J Med Chem. 2001;44:1927–37. doi:10.1021/jm001101a.
68. Winiwarter S, Ax F, Lennernas H, Hallberg A, Pettersson C, Karlen A. Hydrogen bonding descriptors in the prediction of human *in vivo* intestinal permeability. J Mol Graph Model. 2003;21:273–87. doi:10.1016/S1093-3263(02) 00163-8.
69. Bartzatt R. Alkylation activity and molecular properties of two antineoplastic agents that utilise indometacin and a conjugate of aspirin with 2-aminonicotinic acid to transport nitrogen mustard groups. Drugs R D. 2007;8:363–72. doi:10.2165/00126839-200708060-00004.